International Journal of Analysis and Applications

Improved Spatial-Temporal CAR Models for Dengue Fever Incidence: Evidence from Banyumas

Jajang*, Mashuri, Novita Eka Chandra, Budi Pratikno

Department of Mathematics, Faculty of Mathematical and Sciences, Jenderal Soedirman University, Indonesia

**Corresponding author:* jajang@unsoed.ac.id

ABSTRACT. In the last six years, dengue fever cases in Banyumas Regency in 2024 were very high. The relative risk (RR) of dengue hemorrhagic fever (DHF) is of interest. In this paper, we proposed the Spatial Temporal-Conditional Autoregressive (ST-CAR) model to analyze the association of DHF with related factors. In addition, we improve the model with offset modification on ST-CAR. The results of research showed that the best ST-CAR model was the interaction of intrinsic CAR and independent identically distributed temporal effects. In addition, the offset modification in the ST-CAR model resulted in the smallest Watanabe-Akaike Information Criterion (WAIC). Based on the study's findings, the two highest RR from year to year are located not far from the city center (North Purwokerto) and the tourist attraction (Baturaden). Both locations are often associated with higher risk factors such as population density and greater social interaction, which facilitate transmission.

1. Introduction

Relative risk (RR) is a measure commonly used in disease mapping analysis in epidemiology. Spatial disease mapping models borrow power from neighboring units in space, thereby reducing variability in disease risk estimates. The technique is particularly advantageous when studying rare diseases or regions with small populations, which are consistent with the characteristics of counties with missing values, so imputation is based on spatial borrowing power. Usually, this information is presented in regional maps with colors representing the quantitative measure of relative risk. The presentation of RR in regional maps through disease mapping is useful for identifying the geographical distribution of disease burden and disease

Received Sep. 30, 2025

2020 Mathematics Subject Classification. 62M30.

Key words and phrases. dengue hemorrhagic fever; ST-CAR; relative risk; local Getis statistic; WAIC.

https://doi.org/10.28924/2291-8639-23-2025-331

ISSN: 2291-8639

incidence based on risk levels. Studies modelling infectious diseases by mapping the distribution of RR values, known as disease mapping, have been conducted by several researchers previously [1], [2], [3], [4]. Disease mapping aims to capture how the risk is distributed across each region. Clustering relative risk (RR) values in disease mapping is similar to hotspots in general spatial models [5], [6]. Therefore, RR values are important in disease mapping analysis of infectious diseases such as dengue hemorrhagic fever (DHF). To capture spatial independence information in spatial models, a spatial weight matrix component is added. Generally, this matrix has binary elements, namely 1 if two regions share a border and 0 otherwise. The handling of infectious disease problems is certainly not deterministic at a certain point in time; the recognition of trends over time needs to be considered. In terms of information on how spatial effects influence, this is done through an intrinsic conditional autoregressive (ICAR) model, while information on the influence of time is modeled through an autoregressive model.

The lack of freedom in spatial models has implications for model parameter estimation methods. The Bayesian method is an appropriate method that has been extensively studied and applied to spatial model parameter estimation problems. Several studies related to the Bayesian method in conditional autoregressive (ICAR) models can be found in [7], [8], [9], and [10]. The development of the CAR model has also been studied, known as the conditional autoregressive-Besag-York-Mollie (CAR-BYM) model. The CAR-BYM model accommodates spatial and non-spatial effects among regions [11], [12].

In spatial modelling, the weighted matrix is a crucial component in capturing spatial effects, including in CAR models. Spatial matrices generally have values of 1 and 0. The development of spatial weighting matrices has been carried out by Aldstadt and Getis and Jajang et al. [13], [14]. This modification of the spatial weighted matrix combines and utilizes local spatial autocorrelation coefficients and adjacent matrices. Spatial models in epidemiological studies are particularly relevant to the distribution patterns of relative risk in the form of disease mapping. Disease mapping analysis has been extensively studied by various researchers [15]. Disease mapping is the plotting of relative risk (RR) in sub-regions in the form of a map with different color gradations. Through disease mapping, information related to high-risk areas can be analyzed quickly.

Dengue hemorrhagic fever (DHF) is an infectious disease caused by the dengue virus. It is transmitted through the bite of Aedes aegypti or Aedes albopictus mosquitoes that have previously been infected with the dengue virus. Efforts to control this disease cannot be done instantly but must be sustained over a period of several years. To observe the trend of DBD patterns through relative risk in each region, data from several years is required. In epidemiological studies of infectious diseases such as Dengue Hemorrhagic Fever (DHF), using data from only one year is insufficient to understand the dynamics of the disease CAR.

Based on the above description, the motivation for this research is to develop the ST-CAR model through log offset modification and its application to explain the DBD phenomenon in Banyumas Regency from 2019 to 2024. The study was conducted by integrating spatial and temporal aspects through the ST-CAR model. Spatial data is a stochastic process, the realisation of a set of random variables that depend on an index (e.g., field, space, or time index). If D is a region consisting of non-intersecting sub-regions, then the area data type has the characteristic that D is fixed and partitioned into a finite number of area units [16], [17]. The closeness of the relationship between spatial units can be measured by the spatial autocorrelation coefficient. Spatial autocorrelation is related to the non-random patterns of attribute values over a set of spatial units. One measure of spatial correlation is measured by the global or local spatial autocorrelation coefficient.

1.2 Conditional autoregressive models

The conditional autoregressive (CAR) model is one of the spatial modelling techniques often applied in epidemiology [3], [18], [19]. In the context of epidemiology, the description of disease cases is viewed as an aggregate of cases in a region. This aggregate data is generally distributed according to Poisson. The Poisson distribution data is often found in infectious disease modelling problems. Let $Y_i|E_i, \eta_i, i = 1,2, \dots, n$, be random variables following a Poisson distribution, $Y_i \sim POI(E_i e^{\eta_i})$. The link function that relates the Poisson mean and the predictor variable is the log [20], $\log(E_i e^{\eta_i}) = \log(E_i) + \eta_i$, $log(E_i)$ is *offset,* $\boldsymbol{x'_i}$ and the linear predictor, η_i is

$$\eta_i = \alpha + x_i'\beta + v_i, \tag{1}$$

where $\boldsymbol{x}_i' = (x_{1i}, \dots, x_{pi})$, $\beta_1, \dots, \beta_p$ are regression parameters, e^{η_i} denote the risk of disease in area i, and v_i is spatial random effect. The spatial random effects $(v_1, v_2 \dots v_n)$ are modelled by a CAR prior distribution, and its capture any residual spatial autocorrelation in the disease data. Under the *Intrinsic Conditional Autoregressive* (ICAR), $v_i|v_{j\neq i}, W, \tau_I^2 \sim N\left(\frac{1}{\sum_{i\neq j} \mathrm{w}_{ij}} \sum_{i\neq j} \mathrm{w}_{ij} v_j, \frac{\tau_I^2}{\sum_{i\neq j} \mathrm{w}_{ij}}\right)$, where w_{ij} is a weighted matrix element having values one and zero, and $\tau_i w_{ij} = \tau_j w_{ji}$, then $(v_i, v_2, \dots, v_n) \sim MVN(\mathbf{0}, \boldsymbol{Q^{-1}})$. Here, $\boldsymbol{Q}$ is a precision matrix whose elements are (q_{ij}), $q_{ij} = \tau_i w_{ij}$ and $q_{ii} = \tau_i$. Under the convolution model, ε_i is consist of spatial effect and identical and independent distribution (IID), effect. $\varepsilon_i = u_i + v_i$. Therefore, the equation in (1) is

$$\eta_i = \alpha + x_i{}'\beta + u_i + v_i. \tag{2}$$

Poisson distribution data is often found in infectious disease modelling problems, such as dengue haemorrhagic fever (DHF). The involvement of spatial and non-spatial random effects models was proposed by Besag-York-Mollie. Studies of the random effects convolution model $u_i + v_i$ have been conducted by researchers including Besag-York-Mollie [21], [22],[23], [24]. In this case, the focus of modelling is how the log relative risk as a linear combination of predictor variables and random components can capture spatial and/or non-spatial effects.

1.3 Spatial-Temporal conditional autoregressive models

Temporal data, also known as time series or panel data, are data that are seen in a sequential manner based on time. Data with both spatial and temporal aspects is referred to as spatial-temporal data. Spatial-temporal areal data can be seen as a collection of time series that are spatially correlated according to a specific neighboring structure [25]. The Spatial Temporal Conditional Autoregressive (ST-CAR) model is used to handle the time evolution of a simple Conditional Autoregressive (CAR) model [26]. Spatial-temporal conditional autoregressive (ST-CAR) models have been widely used in epidemiology, for example, in cases of dengue hemorrhagic fever (DHF). These models help researchers identify patterns and predict the spread of diseases by taking into account both the spatial distribution of cases and the temporal dynamics of transmission. By integrating various environmental and social factors, ST-CAR models enhance our understanding of disease outbreaks and inform public health interventions. Previous studies of the ST-CAR model have been done by previous researchers [22], [27], [28], [29], [30].

Spatial-temporal disease mapping models are widely used to describe the geographical patterns of a disease and its development over time. In this study, we will apply a spatial-temporal model to understand the temporal development of dengue fever incidence risk at the district level. Various proposals are available for the spatial, temporal, and spatial-temporal interaction components in the model. Interaction is a feature recommended to reflect various patterns of decline and slowdown in different regions and districts [30]. In disease mapping, conditional autoregressive (CAR) models and temporal random effects have been widely applied for spatial and temporal random effects. The spatial-temporal model used is as follows:

$$Y_{it} \sim POI(E_i t e^{\eta_{it}}),$$
$$\eta_{it} = \alpha + x_{it}'\beta + u_i + v_i + \gamma_t + \varphi_t + \delta_{it}, \quad (3)$$

where E_{it} is the number of observations and expectations in area i, at time t, $i = 1,2,\dots,n$ and $t = 1,2,\dots.,T$, α is an overall risk level, β is parameter vector of fixed effect, $u_i, v_i, \gamma_t, \varphi_t$, are spatially unstructured ($u_i|\tau_u^2 \sim N(0,\tau_u^2)$), spatially structured ($v_i$follows ICAR), temporally structured ($\gamma_{t+1} - \gamma_t|\tau_\gamma^2 \sim N(0,\tau_\gamma^2)$), temporally unstructured ($\varphi_t|\tau_\varphi^2 \sim N(0,\tau_\varphi^2)$), respectively, and δ_{it} is the interaction of a pair of the four random effects [19], [31], [32]. Hence, δ_{it} hence captures only the variation that cannot be explained by the main effects. Interaction of a pair of the four random effect is presented by Table 1. Each $\boldsymbol{u}, \boldsymbol{v}, \boldsymbol{\gamma}$, and $\boldsymbol{\varphi}$ are, respectively, assumed multivariate Gaussian with mean zero and precision matrix $\tau^{-2}Q_u, \tau^{-2}Q_v, \tau^{-2}Q_u, \tau^{-2}Q_\gamma$.and $\tau^{-2}Q_\varphi$, where $Q_u = I$, and $Q_\varphi = I$,

$$Q_v = (q_{ij}), q_{ij} = \begin{cases} -1, & i \sim j \\ n_i, & i = j \\ 0, & \text{otherwise} \end{cases},$$

$$Q_\gamma = (q_{ij}), q_{ij} = \begin{cases} -1, & i = j+1, i = j-1, \quad i,j = 2,..,T-1 \\ 1, & i = j, \quad \text{i,j} = 1,\text{T} \\ 2, & \text{i} = \text{j}, \ \text{i,j} = 2,\dots,\text{T}-1. \end{cases}$$

Table 1. Five ST-CAR models according to the type of interaction

Type	Model	Precision Matrix of interaction	description
I	$\eta_{it} = X'_{it}\beta + u_i + v_i + \gamma_t + \varphi_t$	-	-
II	$\eta_{it} = X'_{it}\beta + u_i + v_i + \gamma_t + \varphi_t + \delta_{it}$	$Q_\delta = I \otimes I$	spatial and temporal effects are both independent and identically distributed
III	$\eta_{it} = X'_{it}\beta + u_i + v_i + \gamma_t + \varphi_t + \delta_{it}$	$Q_\delta = I \otimes Q_\gamma$	spatial effect is independent and temporal effects is AR1
IV	$\eta_{it} = X'_{it}\beta + u_i + v_i + \gamma_t + \varphi_t + \delta_{it}$	$Q_\delta = Q_v \otimes I$	spatial effect is ICAR and temporal effects are independent and identically distributed.
V	$\eta_{it} = X'_{it}\beta + u_i + v_i + \gamma_t + \varphi_t + \delta_{it}$	$Q_\delta = Q_v \otimes Q_\gamma$	Spatial effect is ICAR and temporal effects is AR1

1.4 Local Getis statistic.

The local Getis statistic is a measure of spatial autocorrelation that can be used for spatial clustering of objects. Spatial clustering patterns can often provide more information than a global overview. The local Getis statistic is defined as

$$G_i = \frac{\sum_j w_{ij}x_j}{\sum_j x_j}, \ \text{j} \neq \text{i} \tag{4}$$

where w_{ij} are the elements of the symmetric spatial weighting matrix that have values 1 and 0. The mean and variance of the G_i statistic under the null hypothesis are $E(G_i) = \frac{w_i}{n-1}$ and $Var(G_i) = \frac{w_i(n-1-w_i)}{(n-1)^2(n-2)} \cdot \left[\frac{s(i)}{\bar{x}(i)}\right]^2$, $\bar{x}(i) = \frac{\sum_j x_j}{n-1}$ dan $s^2(i) = \frac{\sum_j x_j^2}{n-1} - \left(\bar{x}(i)\right)^2$. Therefore, based on the mean value and variance, the standardized local Getis statistic is $G_i^* = \frac{G_i - E(G_i)}{\sqrt{Var(G_i)}}$.

2. Material and Method

Banyumas is one of the residences in Central Java Province with a fairly high number of dengue fever cases. Banyumas consists of twenty-seven districts.

Given the high number of dengue fever cases in Banyumas, this research is interesting to examine. The research variables used in this study are the total number of dengue fever cases (persons) and several predictor variables. These predictor variables are altitude (above sea level), population density (persons/km²), hospitals (total units of hospital), integrated health posts, public health centers, public health officers, environmental health officers, and overall sanitation.

From 2019 to 2024, secondary data on dengue hemorrhagic fever (DHF) from the Central Statistics Agency (BPS) and the Banyumas Health Office (DINKES) were utilized in this study.

The analysis method consists of two parts, namely descriptive analysis and inferential analysis using the ST-CAR model. The initial stage involves descriptive analysis of DBD data using numerical summaries and thematic maps. The use of plot maps is intended to obtain information on the number of DBD cases quickly. The next descriptive analysis is to measure spatial closeness through local Getis statistics. Finally, we use ST-CAR to investigate the trend in the number of cases from year to year through long time series to see the time trend to see the trend in the number of cases from year to year. This study examines standard models, model modifications, and model implementation.

3. Results and Discussion

3.1 Description of research variables

Descriptive statistics is the initial stage in modeling, namely, data exploration. Table 2 presents descriptive statistics of the number of dengue hemorrhagic fever (DHF) cases and variables related to the number of DHF cases. In statistical modeling, the type of response variable is closely related to the model selected. In the case of the number of DHF cases, the appropriate data type is count data, and more specifically, the Poisson distribution.

Table 2. Descriptive Statistics of the total cases of DHF and its Predictor Variables

Variable	N	mean	sd	Median	min	max
Total cases	162	22.24	30.55	10.50	0	139
Density	162	2103.38	1839.71	1386	486	7377
Altitude	162	108.03	107.76	74	15	420
hospital	162	0.61	0.95	0	0	3
integrated health post	162	94.53	28.19	91	50	181
Public Health center	162	3.28	3.88	2	1	28
Environmental Health Officer	162	4.08	2.24	4	1	11
Public Health Officer	162	3.21	1.90	3	0	12
Sanitation	162	20128.41	7305.01	18818	4261	44646

Based on Table 2, it can be explained that there were a total of 27 cases, and observations were conducted over six years, bringing the total observations to 162. The average number of cases from twenty-seven districts over six years was 22.24 with a standard deviation of 30.56. The magnitude of the standard deviation is influenced by variations between regions and between years during the observation. Meanwhile, the median is 10.5, almost half the average. This

indicates that in recent years (2024), the number of cases has been very high. The minimum value is 0, and the maximum is 139, so the total range of cases in Banyumas Regency is very high.

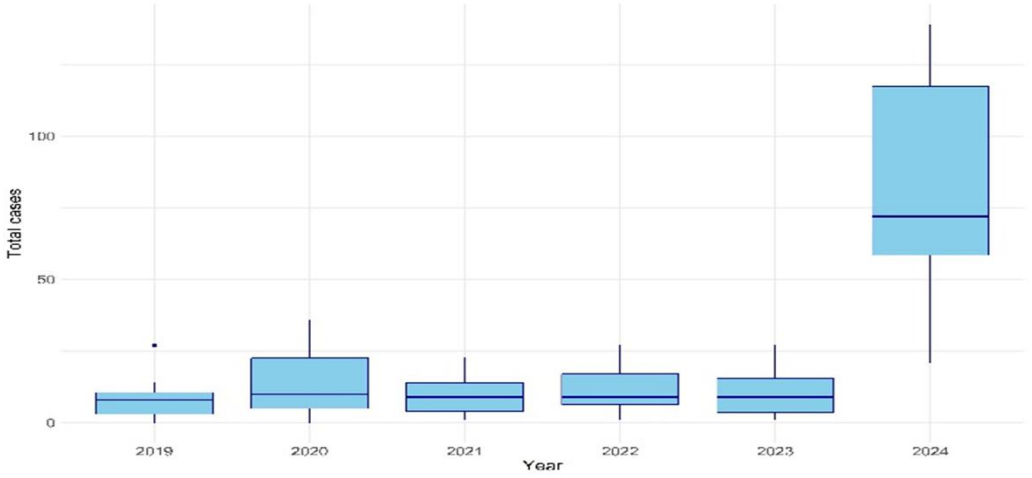

Figure 1. Boxplot of the number of DHF Cases in Banyumas Regency 2019-2024

Figure 1 shows boxplots (box-and-whisker plots) of the number of dengue fever cases per district in Banyumas from 2019 to 2024. Based on Figure 1, it appears that the number of cases from 2019 to 2023 does not show a significant increase. The third quartile value is below 20, while the median value from year to year tends to be evenly distributed around 10. However, a fairly extreme increase occurred in 2024. The minimum number of DHF cases in 2024 exceeds the average third quartile value in each of the previous years (2019 to 2023). This is noteworthy because these cases occurred in all districts.

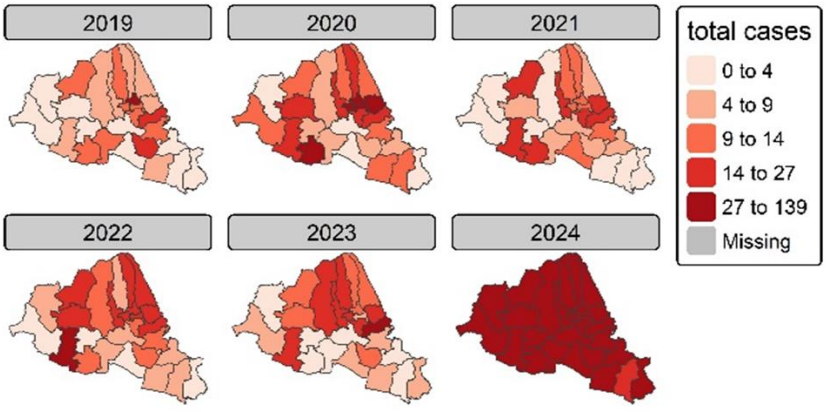

Figure 2. Mapping the number of DHF cases per district in Banyumas Regency, 2019-2024.

Figure 2 shows disease mapping of the number of dengue fever cases per district in Banyumas Regency from 2019 to 2024. The spatial distribution pattern of dengue fever cases from 2019 to 2023 has similar characteristics, especially from 2020 to 2023. However, in 2024, there was a significant increase in dengue fever cases. The number of cases increased across all districts, as indicated by the dark brown color in the area. The significant surge in 2024 warrants serious attention and in-depth study regarding several patterns of community behavior, government response, weather conditions in 2024, and several related factors. The total number of cases from 2019 to 2024 can be seen in Figure 3.

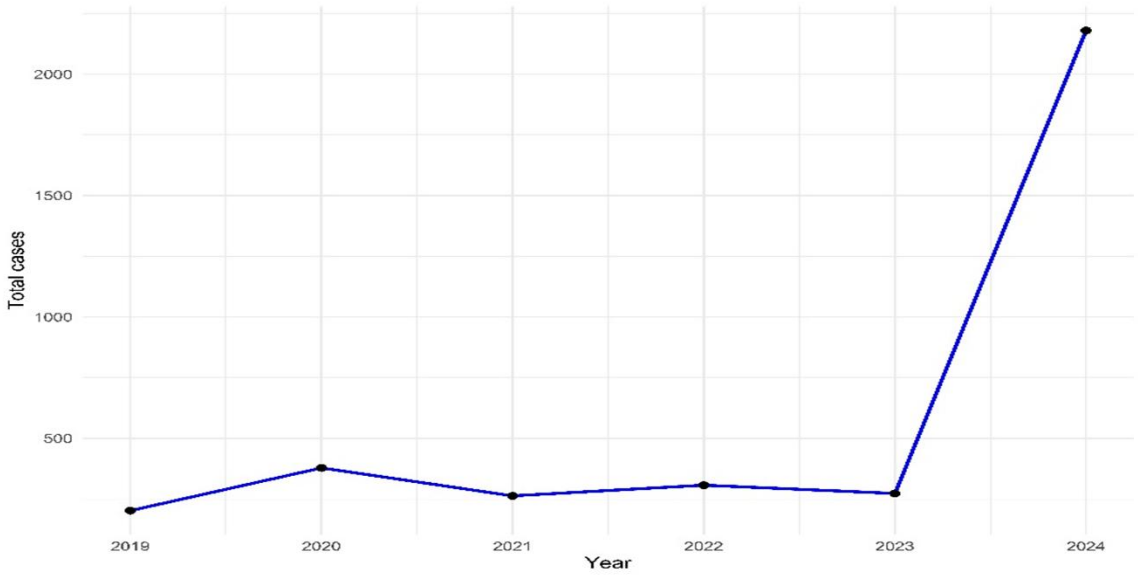

Figure 3. Trend of DHF cases in Banyumas 2019-2024.

Another interesting piece of information from Figure 3 is the total number of cases from 27 districts, which is extremely high. From 2019 to 2023, the number of cases in Banyumas Regency was around 500 people, but in 2024 it exceeded 2,000. This means that the total number of cases in 2024 is more than four times higher than in previous years. The overview of the number of cases per district through disease mapping as shown in Figure 1, shows variations among districts. The total number of cases within the given range shows that the mapping of the number of cases in 2024 is all dark orange. Meanwhile, for the number of cases from 2019 to 2023, there appears to be a correlation, forming clusters based on the degradation of color from light to dark.

3.2 Fitting Spatial-Temporal Conditional Autoregressive

The local Getis statistic value is calculated annually to observe the characteristics between districts in the same year. The results of the G_i^* value calculation are then presented or mapped to make them more informative. The standardized local Getis statistic values are presented in Figure 3. Based on Figure 4, it appears that several regions have a relatively stable

trend compared to other regions. Values below zero (negative) are colored purple with increasing color degradation as the G_i^* statistical value decreases. This means that areas with fewer cases compared to other regions will be marked with a darker shade of purple.

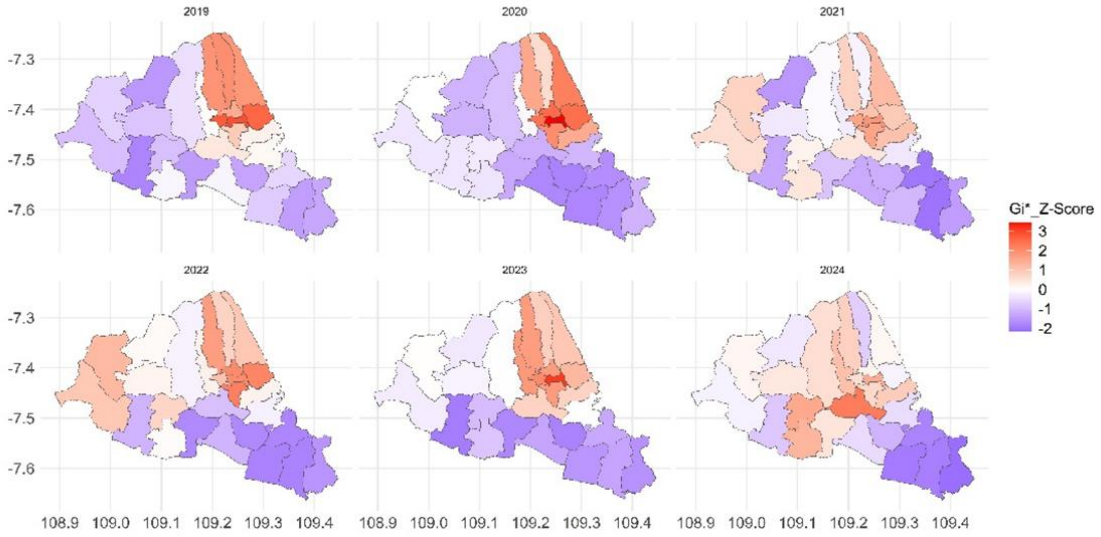

Figure 4. The distribution of the local Getis statistic of DHF cases 2019-2024.

Based on the information in Figure 3 and Figure 4, there appears to be spatial grouping based on the total cases and local Getis statistic values. Referring to this information, the offset component in the ST-CAR model is modified. The modified Eit is obtained by calculating the surrounding observations resulting from spatial clustering using the local Getis statistic. Let $Y_{it}|E_{it},\eta_{it}\sim Poi(E_{it}e^{\eta_{it}})$, η_{it} is the linear predictor, and E_{it} is the expected number of cases in region i in year t, $E_{it} = n_{it}\frac{\left(\sum_{j=1}^{n_t} y_{jt}\right)}{\left(\sum_{j=1}^{n_t} n_{jt}\right)}$. The E_{it} modification of the ST-CAr model was carried out by creating clusters based on the quantile values of the G^* statistic. Variations in quantile-p and WAIC results are presented in Table 5. The ST-CAR model was created into several model scenarios and expectation calculations according to clusters. Observations for each year are grouped into three clusters: below the quantile (q), above the (1-q), and in between. Next, the expected value is calculated for each cluster formed. These values are calculated using the formula $E_{itk} = n_{itk}\frac{\left(\sum_{j\in c_k} y_{jtk}\right)}{\left(\sum_{j\in c_k} n_{jtk}\right)}$, then E_{it} is obtained from the combined results, $E_{it} = E_{it1} \cup E_{it2} \cup E_{it3}$. Table 3 presents the WAIC values for the ST-CAR model at various quantile values. The quantile values used are 0%, 5%, 10%, 15%, ..., and 35%.

Table 3. Comparison of DIC and WAIC of ST-CAR and Modification Offset

quantile	M	DIC	WAIC	quantile	M	DIC	WAIC
	Model I	1.177.17	1.276.67		Model I	1.141.75	1.212.04
	Model II	966.64	955.58		Model II	965.31	954.71
0	Model III	975.32	969.76	20%	Model III	976.96	976.67
	Model IV	965.57	964.82		Model IV	960.52	961.36
	Model V	973.64	978.95		Model V	967.17	972.94
	Model I	1.189.10	1.276.40		Model I	1.170.44	1.265.60
	Model II	967.83	956.51		Model II	965.31	954.67
5%	Model III	980.86	980.23	25%	Model III	974.77	972.75
	Model IV	968.03	967.95		Model IV	957.44	955.66
	Model V	980.86	991.53		Model V	963.55	966.13
	Model I	1.175.09	1.255.28		Model I	1.165.24	1.254.49
	Model II	965.31	954.68		Model II	965.31	954.70
10%	Model III	979.93	978.24	30%	Model III	969.78	967.00
	Model IV	967.18	968.13		Model IV	**953.23**	**950.64**
	Model V	982.20	996.48		Model V	960.57	962.90
	Model I	1.189.10	1.276.40		Model I	1.195.78	1.307.22
	Model II	965.31	954.68		Model II	965.31	954.70
15%	Model III	980.86	980.22	35%	Model III	976.18	975.12
	Model IV	968.03	967.95		Model IV	961.10	959.95
	Model V	980.89	991.29		Model V	968.95	974.19

Based on Table 3, the effect of grouping objects (districts) on changes in WAIC value appears to be significant. Based on the WAIC values in Table 3, the minimum WAIC value is model IV at the 30% quantile, with a WAIC value of 950.64.

The next DHF modeling is to use a type IV model with a quantile value of 30% or 0.3. The results of the estimation of the mean, $q_{0.025}$ (0.025quant), $q_{0.025}$ (0.5quant), $q_{0.975}$ (0.975quant) of the predictor variables are presented in Table 4. Here, some variables such as density, height, and sanitation are scaled to avoid too much variability. The Watanabe-Akaike Information Criterion (WAIC) value of this model is 950.64 (bottom of Table 4). To measure the accuracy of the model, the next step is to plot the actual data and the predicted results.

Table 4. Fixed and random effects of ST-CAR model

Fixed	mean	0.025quant	0.5quant	0.975quant
Intercept	0.3021	-70.0126	0.3022	70.6161
Density (10^2)	-0.0356	-0.1488	-0.0357	0.0780
Altitude (10)	-0.0047	-5.0719	-0.0048	5.0626
Hospital	-0.2091	-0.5473	-0.2082	0.1243
integrated health post	0.0006	-0.0083	0.0007	0.0096
Public Health Centers	0.0021	-0.0200	0.0020	0.0243
Environmental Health Officer	0.0203	-0.0420	0.0204	0.0821
Public Health Officer	0.0370	-0.0123	0.0370	0.0859
Sanitation (10^4)	0.1361	-0.1166	0.1364	0.3869
Random				
Spatial unstructured	110.94	7.48	72.80	434.36
Spatial structured	1105.83	73.85	724.57	4335.55
Time structured	21907.09	1440.95	14348.88	85812.02
Time unstructured	21875.70	1427.14	14289.41	85959.82
Interaction	11.01	6.53	10.66	17.47

Watanabe-Akaike information criterion (WAIC): 950.64

The scatter plot of actual and predicted is presented in Figure 5. The plot of points (scatter plot) of actual and predicted in Figure 5 shows the predictions and actual values at the 30th quantile with the addition of a dummy variable

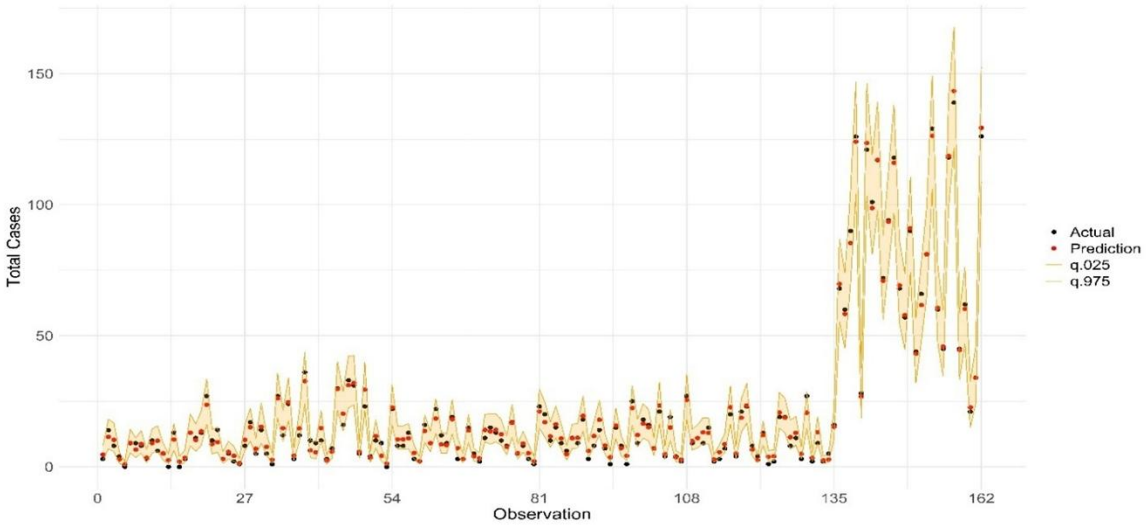

Figure 5. Plot of the Number DHF of Predicted and Actual 2019-2024

After obtaining the best model and model coefficients listed in Table 4, the next step is to determine the relative risk (RR) value. Based on model IV in Table 1 and the estimator values or coefficients of the fixed and random models in Table 4, the estimator for $\hat{\eta}_{it}$is obtained, and finally, from η_{it} we obtain RR_{it}. The RR mapping for each district in Banyumas from 2019 to 2024 can be seen in Figure 6.

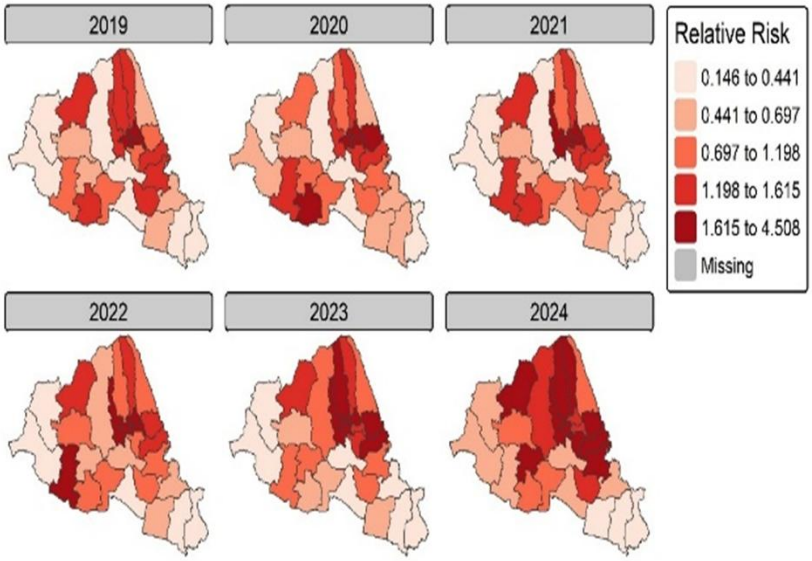

Figure 6. Relative Risk Distribution resulting from the ST-CAR model IV.

RR is the ratio of observation to expectation. The highest RR values from year to year (2019 to 2024) are North Purwokerto (2.727), Jatilawang (1.978), Karanglewas (2.184), Wangon (2.238), Baturaden (2.021), and Baturaden (3.708), respectively. A highest RR of 3.708 means the risk in the district is approximately 3.708 times greater than expected. The districts with the highest RR values from year to year are located not far from the city center, namely North Purwokerto and the tourist attraction (Baturaden). Locations close to city centers are often associated with higher risk factors such as population density, mobility centers, crowds, and greater social interaction, which facilitate transmission.

Conclusion

Between 2019 and 2024, the number of dengue fever cases in Banyumas Regency experienced an extreme spike in 2024. Identification efforts can be conducted in various ways, one of which is identifying factors associated with dengue fever cases. Therefore, modelling that can accommodate spatial and temporal random effects is necessary. The Spatial Temporal Conditional Autoregressive model can simultaneously explain and identify variations between regions and over time.

Modelling using ST-CAR for dengue cases focuses on the distribution of relative risk patterns in surrounding areas. Therefore, spatial clustering, which refers to local spatial measures through local Getis statistics related to this case, is used. Spatial clustering and log offset modification in the ST-CAR model for dengue cases provide improved accuracy. This is indicated by a decrease in the Watanabe Akaike Information Criteria (WAIC) value.

The districts with the highest year-to-year changes are located not far from the city center. Therefore, we conclude that the locations close to city centers are often associated with higher risk factors such as population density, mobility centers, crowds, and greater social interaction, which facilitate transmission.

Acknowledgment: The authors would like to thank the Institute for Research and Community Service (LPPM) of Jenderal Soedirman University with contract number Nomor:16.63/UN23.34/PT.01/V/2025. Secondly, the authors would like to thank the Central Statistics Agency (BPS) of Central Java and the Health Office for publishing data to support our research

Conflicts of Interest: The authors declare that there are no conflicts of interest regarding the publication of this paper.

References

[1] D. Lee, A. Rushworth, S.K. Sahu, A Bayesian Localized Conditional Autoregressive Model for Estimating the Health Effects of Air Pollution, Biometrics 70 (2014), 419-429. https://doi.org/10.1111/biom.12156.

[2] A. Aswi, S. Cramb, E. Duncan, K. Mengersen, Evaluating the Impact of a Small Number of Areas on Spatial Estimation, Int. J. Health Geogr. 19 (2020), 39. https://doi.org/10.1186/s12942-020-00233-1.

[3] M.R. Desjardins, M.D. Eastin, R. Paul, I. Casas, E.M. Delmelle, Space–Time Conditional Autoregressive Modeling to Estimate Neighborhood-Level Risks for Dengue Fever in Cali, Colombia, Am. J. Trop. Med. Hyg. 103 (2020), 2040-2053. https://doi.org/10.4269/ajtmh.20-0080.

[4] A. Wubuli, F. Xue, D. Jiang, X. Yao, H. Upur, et al., Socio-Demographic Predictors and Distribution of Pulmonary Tuberculosis (TB) in Xinjiang, China: A Spatial Analysis, PLOS ONE 10 (2015), e0144010. https://doi.org/10.1371/journal.pone.0144010.

[5] S. Mclafferty, Disease Cluster Detection Methods: Recent Developments and Public Health Implications, Ann. GIS 21 (2015), 127-133. https://doi.org/10.1080/19475683.2015.1008572.

[6] T.A. Nelson, B. Boots, Detecting Spatial Hot Spots in Landscape Ecology, Ecography 31 (2008), 556-566. https://doi.org/10.1111/j.0906-7590.2008.05548.x.

[7] S. Ahmed, A. Hussein, M. Al-Momani, Efficient Estimation for the Conditional Autoregressive Model, J. Stat. Comput. Simul. 85 (2014), 2569-2581. https://doi.org/10.1080/00949655.2014.893346.

[8] Q. Zeng, H. Wen, S. Wong, H. Huang, Q. Guo, et al., Spatial Joint Analysis for Zonal Daytime and Nighttime Crash Frequencies Using a Bayesian Bivariate Conditional Autoregressive Model, J. Transp. Saf. Secur. 12 (2018), 566-585. https://doi.org/10.1080/19439962.2018.1516259.

[9] X. Han, L. Lee, Bayesian Estimation and Model Selection for Spatial Durbin Error Model with Finite Distributed Lags, Reg. Sci. Urban Econ. 43 (2013), 816-837. https://doi.org/10.1016/j.regsciurbeco.2013.04.006.

[10] J. Hendricks, C. Neumann, A Bayesian Approach for the Analysis of Error Rate Studies in Forensic Science, Forensic Sci. Int. 306 (2020), 110047. https://doi.org/10.1016/j.forsciint.2019.110047.

[11] Y. Cheng, J. Norris, C. Bao, Q. Liang, J. Hu, et al., Geographical Information Systems-Based Spatial Analysis and Implications for Syphilis Interventions in Jiangsu Province, People's Republic of China, Geospat. Health 7 (2012), 63. https://doi.org/10.4081/gh.2012.105.

[12] Z. Peng, Y. Cheng, K.H. Reilly, L. Wang, et al., Spatial Distribution of HIV/AIDS in Yunnan Province, People's Republic of China, Geospat. Health 5 (2011), 177. https://doi.org/10.4081/gh.2011.169.

[13] J. Aldstadt, A. Getis, Using AMOEBA to Create a Spatial Weights Matrix and Identify Spatial Clusters, Geogr. Anal. 38 (2006), 327-343. https://doi.org/10.1111/j.1538-4632.2006.00689.x.

[14] Jajang, B. Pratikno, M. Nusrang, Analysis of the W-Amoeba Getis and Moran on Spatial Dynamic Panel Models, Far East J. Math. Sci. 102 (2017), 655-667. https://doi.org/10.17654/ms102040655.

[15] A. Adin, T. Goicoa, M.D. Ugarte, Online Relative Risks/rates Estimation in Spatial and Spatio-Temporal Disease Mapping, Comput. Methods Programs Biomed. 172 (2019), 103-116. https://doi.org/10.1016/j.cmpb.2019.02.014.

[16] N. Cressie, Statistics for Spatial Data, John Wiley & Sons, 2015.

[17] S. Banerjee, B.P. Carlin, A.E. Gelfand, S. Banerjee, Hierarchical Modeling and Analysis for Spatial Data, Chapman and Hall/CRC, 2003. https://doi.org/10.1201/9780203487808.

[18] K. Ben-Ahmed, A. Bouratbine, M. El-Aroui, Generalized Linear Spatial Models in Epidemiology: A Case Study of Zoonotic Cutaneous Leishmaniasis in Tunisia, J. Appl. Stat. 37 (2009), 159-170. https://doi.org/10.1080/02664760802684169.

[19] Y. Wang, X. Chen, F. Xue, A Review of Bayesian Spatiotemporal Models in Spatial Epidemiology, ISPRS Int. J. Geo-Inf. 13 (2024), 97. https://doi.org/10.3390/ijgi13030097.

[20] P. McCullagh, Generalized Linear Models, Routledge, 2019.

[21] J. Besag, Spatial Interaction and the Statistical Analysis of Lattice Systems, J. R. Stat. Soc. Ser. B: Stat. Methodol. 36 (1974), 192-225. https://doi.org/10.1111/j.2517-6161.1974.tb00999.x.

[22] D. De Witte, A.A. Abad, G. Molenberghs, G. Verbeke, L. Sanchez, et al., A Multivariate Spatio-Temporal Model for the Incidence of Imported COVID-19 Cases and COVID-19 Deaths in Cuba, Spat. Spatio-temporal Epidemiol. 45 (2023), 100588. https://doi.org/10.1016/j.sste.2023.100588.

[23] M. Morris, K. Wheeler-Martin, D. Simpson, S.J. Mooney, A. Gelman, et al., Bayesian Hierarchical Spatial Models: Implementing the Besag York Mollié Model in Stan, Spat. Spatio-temporal Epidemiol. 31 (2019), 100301. https://doi.org/10.1016/j.sste.2019.100301.

[24] J. Jajang, B. Pratikno, M. Mashuri, I.E. Cahyarini, The Dengue Hemorrhagic Fever Modeling in Banyumas Regency by Using Car-Bym, Generalized Poisson, and Negative Binomial, in: Advances in Physics Research, Atlantis Press, Paris, France, 2022. https://doi.org/10.2991/apr.k.220503.007.

[25] A. Mozdzen, A. Cremaschi, A. Cadonna, A. Guglielmi, G. Kastner, Bayesian Modeling and Clustering for Spatio-Temporal Areal Data: An Application to Italian Unemployment, Spat. Stat. 52 (2022), 100715. https://doi.org/10.1016/j.spasta.2022.100715.

[26] L. Mariella, M. Tarantino, Spatial Temporal Conditional Auto-Regressive Model: A New Autoregressive Matrix, Austrian J. Stat. 39 (2016), 223-244. https://doi.org/10.17713/ajs.v39i3.246.

[27] A. Aswi, S. Rahardiantoro, A. Kurnia, B. Sartono, D. Handayani, et al., Bayesian Spatio-Temporal Conditional Autoregressive Localized Modeling Techniques for Socioeconomic Factors and Stunting in Indonesia, MethodsX 15 (2025), 103464. https://doi.org/10.1016/j.mex.2025.103464.

[28] A. Adin, T. Goicoa, M.D. Ugarte, Online Relative Risks/rates Estimation in Spatial and Spatio-Temporal Disease Mapping, Comput. Methods Programs Biomed. 172 (2019), 103-116. https://doi.org/10.1016/j.cmpb.2019.02.014.

[29] S.K. Sahu, D. Böhning, Bayesian Spatio-Temporal Joint Disease Mapping of COVID-19 Cases and Deaths in Local Authorities of England, Spat. Stat. 49 (2022), 100519. https://doi.org/10.1016/j.spasta.2021.100519.

[30] A. Urdangarin, T. Goicoa, P. Congdon, M. Ugarte, A Fast Approach for Analyzing Spatio-Temporal Patterns in Ischemic Heart Disease Mortality Across US Counties (1999–2021), Spat. Spatio-Temp. Epidemiol. 52 (2025), 100700. https://doi.org/10.1016/j.sste.2024.100700.

[31] L. Knorr-Held, Bayesian Modelling of Inseparable Space-Time Variation in Disease Risk, Stat. Med. 19 (2000), 2555-2567. https://doi.org/10.1002/1097-0258(20000915/30)19:17/18<2555::aid-sim587>3.0.co;2-#.

[32] M. Blangiardo, M. Cameletti, G. Baio, H. Rue, Spatial and Spatio-Temporal Models with R-Inla, Spat. Spatio-Temp. Epidemiol. 4 (2013), 33-49. https://doi.org/10.1016/j.sste.2012.12.001.